

# $W + \text{CHARM}$ PRODUCTION WITH MASSIVE $c$ QUARKS IN PowHel\*

G. BEVILACQUA

ELKH-DE Particle Physics Research Group  
4010 Debrecen, P.O. Box 105, Hungary

M.V. GARZELLI

II. Institute for Theoretical Physics, Hamburg University  
Luruper Chaussee 149, 22761 Hamburg, Germany

A. KARDOS, L. TOTH

Department of Experimental Physics, Institute of Physics  
Faculty of Science and Technology, University of Debrecen  
4010 Debrecen, P.O. Box 105, Hungary

*Received 23 December 2021, accepted 28 December 2021,  
published online 28 February 2022*

Precise calculations for the Large Hadron Collider cannot be imagined without precise parton density functions. For accurate measurements and comparisons, both the valence- and sea-quark parton density functions are needed with high confidence. The hadroproduction of a  $W$  vector boson with a massive charm quark plays an important role in the determination of sea-quark parton density functions because it provides a direct way to measure strangeness in the proton. In this paper, we obtain a next-to-leading order prediction for  $W$ -boson production in association with a  $c$  quark in QCD and match our results to parton shower and hadronization models using PYTHIA 8 in order to get predictions at the hadron level. Our particle-level predictions are compared against available experimental results done by both the ATLAS and CMS collaborations.

DOI:10.5506/APhysPolBSupp.15.2-A8

## 1. Introduction

The end of Run 2 of the Large Hadron Collider (LHC) closes a very successful data acquisition period. During Run 2, it was possible to collect a

---

\* Presented at the XLIV International Conference of Theoretical Physics “Matter to the Deepest”, 15–17 September, 2021.

huge amount of data with high accuracy. For precision tests of the Standard Model and for the quest of searching for new physics, these high-quality data should be compared to the state-of-the-art theoretical predictions. High accuracy in a theoretical calculation can only be achieved if all ingredients are well under control. For a theoretical prediction the statistical accuracy of the involved Monte-Carlo integrations, and the accuracy of the approximation, *i.e.* the order of the various perturbative expansions up to which contributions are taken into account, are usually regarded. For the LHC, being a hadron–hadron collider, the parton density functions (PDFs) play an important role in prediction making. Since perturbation theory is applied to the parton level, cross sections for processes at hadron colliders can only be expressed in terms of a convolution with PDFs as stated by the factorization theorem.

While all the other elements of a prediction can be, in principle, improved by including more terms in the perturbative expansion, by better algorithms for Monte-Carlo integration, *etc.*, the only possible way to improve the accuracy of the used PDFs is by more accurate measurements since these cannot be obtained from first principles. The determination of PDFs generally relies upon fitting procedures based on different processes measured with high accuracy at various colliders. In particular, PDF fits greatly rely on Deep Inelastic Scattering (DIS) data recorded at HERA. A big part of PDF uncertainty is coming from sea-quark distributions for which measurements had a limited accuracy. To decrease uncertainty for these distributions, several plans exist such as the Large Hadron–Electron Collider [1] and at the planned Forward Physics Facility [2] at the High-Luminosity LHC.

For the time being, while these new facilities are being designed and built, the sea-quark content of the proton can be further constrained by making precise predictions for processes at the LHC which are sensitive to sea-quarks and use them in various PDF fits. Particularly interesting in this respect is the associated hadroproduction of a  $W$  boson with a charm quark. For this process, possible final states are restricted by charge conservation and at the lowest order, this yields to the processes of  $pp \rightarrow W^+ \bar{c}$  and  $pp \rightarrow W^- c$ <sup>1</sup>. Thus,  $Wc$  production is an excellent candidate for refining the sea-quark content of the proton since the dominant partonic subprocesses at the Born level have an anti-strange or strange quark in the initial state. Beside their use in refining sea-quark PDFs, these processes can also be used in BSM searches as Standard Model backgrounds.

The importance of this process in PDF fits and in BSM searches is well-recognized. The cross section for the associated production of  $W$  with a massive charm is calculated at the parton level with NLO QCD effects for

---

<sup>1</sup> For brevity, we are going to refer to these processes as  $Wc$ .

the first time in Ref. [3], later implemented in MCFM [4], hadron level predictions were made with the MC@NLO matching with massless charms [5], and recently the first NNLO QCD prediction has been published using a massless charm [6].

The possible key uses of this process have been recognized by the experimentalist community as well. The first measurements for these final states were carried out at the Tevatron by the CDF and D0 collaborations [7–9]. Their measurements were restricted to obtain cross sections for charmed-jet ( $j_c$ ) production due to limited data. These investigations were continued at the LHC by two experiments both at 7 TeV (ATLAS and CMS) and at 13 TeV (CMS). Due to the amount of data available, not only associated charmed-jet production but also associated  $D$ -meson production was analyzed [10–12].

In this work, we summarize our implementation of the  $Wc$  process with a massive  $c$  quark in the PowHel framework which can provide hadron-level predictions for this process with NLO QCD accuracy by performing a match to parton shower algorithms using the POWHEG matching framework [13–15] and PYTHIA 8 [16] for parton shower and hadronization.

## 2. The calculational framework

To obtain hadron-level predictions, the PowHel numerical code is used which utilizes POWHEGBOX-v2 [15] to perform the POWHEG matching to parton showers. To achieve the NLO QCD accuracy, several tree- and one-loop squared matrix elements are needed, these are provided by the HELAC-NLO [17] numerical program.

In order to model the process with the utmost precision, the charm quark is treated massive with mass being user-configurable via the `cmass` reserved word in the input card. The  $W$  boson sign can be chosen with the `vmode` parameter:  $W^+ = +24$ ,  $W^- = -24$ . The possible lepton decay channels can be parameterized via the `vdecaymode` reserved word: `vdecaymode = 100 ·  $n_e$  + 10 ·  $n_\nu$  +  $n_\tau$`  with  $n_i$  equal to 1 (0) if the actual channel is allowed (turned off). The vector boson can be produced in the narrow width approximation (`nwa 1`) or completely off-shell (`nwa 0`) with the mass window specified via the `mlo` and the `mhigh` reserved words with the argument being the corresponding limit energy in GeV.

By default, we consider all leptonic decay channels (`vdecaymode 111`) with complete off-shell effects (`nwa 0`) and a mass window such that  $s_W \in \{30^2, 400^2\}$  GeV<sup>2</sup> (`mlo 30d0` and `mhigh 400d0`). One more option is offered for the user affecting event generation: it is possible to generate events without spin correlations in the vector-boson decay product. In this case,

the kinematics of the lepton pair produced in the  $W$  decay is completely isotropic in the rest frame of the  $W$  and boosted accordingly. This setup can be activated by putting a line containing `nospin 1` in the input card.

Various PDFs can use different values of  $\Lambda_{\text{QCD}}$ , hence to make changes easy for this parameter, a reserved word is provided for it to be able to change it from the input card: by putting the `qcd15` keyword in the input card with a number the corresponding numerical value will be taken as the  $\Lambda_{\text{QCD}}$  as expressed in GeVs.

To speed up event generation, the process is equipped with a `fakevirt` option: if it is present with a numerical argument, the virtual contribution is replaced during the computation with the Born squared matrix element multiplied by this number. To get the correct cross section and event weight after event generation, an event reweight has to be performed with altering the input card by including line containing `compute_rwgt 1`. By running the code with this option active upon execution, the program asks for the event file needed to be reweighted.

For the optimal event generation efficiency and the Sudakov peak formation in the transverse momentum distribution of the extra radiation, the `flg_bornzerodamp` option of POWHEGBOX-v2 is activated. This is the only parameter which was needed to set in order to get coincidence between fixed-order and matched predictions for high- $p_{\text{T}}$  of the radiated massless parton in the real-emission contribution.

### 3. Results

In order to make predictions for this process, several parameters have to be set. These are listed in Table 1. To obtain the complete set of electroweak parameters, the  $G_{\mu}$  scheme was employed obtaining the electromagnetic coupling using

$$\alpha = \frac{\sqrt{2}}{\pi} G_{\text{F}} m_{\text{W}}^2 \sin^2 \theta_{\text{W}}, \quad (1)$$

Table 1. Standard Model parameters used in the runs.

Parameter	Value	Parameter	Value
$\sin^2 \theta_{\text{Cabibbo}}$	0.050934360	$\Gamma_{\text{W}}$	2.085 GeV
$G_{\text{F}}$	$1.16639 \times 10^{-5} \text{ GeV}^{-2}$	$m_{\text{c}}$	1.5 GeV
$M_{\text{W}}$	80.379 GeV	$m_{\text{b}}$	4.75 GeV
$M_{\text{Z}}$	91.1876 GeV	$m_{\text{t}}$	172.5 GeV

where the Weinberg angle is calculated from the vector boson masses

$$\sin^2 \theta_W = 1 - \frac{m_W^2}{m_Z^2}. \quad (2)$$

As for the non-physical scales, the factorization and renormalization scales, several choices were tried out and an optimal scale uncertainty resulted from making the two scales coincide and equal to  $H_T/2$ , such that

$$H_T = \sqrt{p_{T,W}^2 + m_W^2} + \sqrt{p_{T,c}^2 + m_c^2}, \quad (3)$$

where  $p_{T,W}$  and  $p_{T,c}$  are the transverse momenta for the vector boson and the charm quark, respectively. In an NLO calculation, final states with different parton multiplicities are involved, hence in our case, the scales are evaluated with the underlying Born kinematics. For all our scale uncertainty studies to determine the total uncertainty coming from the variation of non-physical scales, both scales were varied such that  $\mu_R = \xi_R H_T/2$  and  $\mu_F = \xi_F H_T/2$  with  $\xi_R, \xi_F \in \{1/2, 2\}$ , and the antipodal configurations left out.

### 3.1. Role of off-shellness and spin correlations

Before turning into phenomenological results, we investigated both the role of spin correlations in vector-boson decay and the effect of off-shellness of the produced vector boson. To study the effect and the impact of these effects, four different scenarios were analyzed and corresponding sample distributions were made and depicted in Fig. 1. Since the sole purpose of this study is to get an idea of the size and impact of the above-mentioned effects,

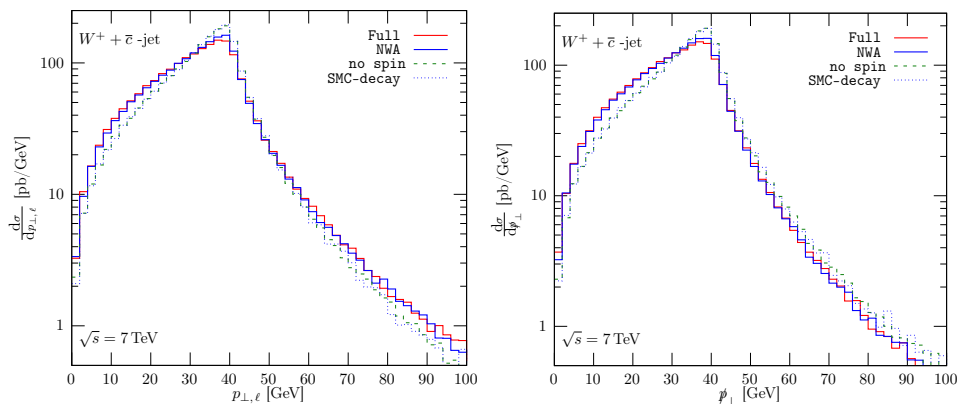


Fig. 1. Lepton transverse momentum (left-hand side) and missing transverse momentum (right-hand side) distributions at 7 TeV for various setups. See the main text for details.

a fully inclusive event sample was generated at 7 TeV for  $W^+ \bar{c}$  using our default scale and the ABMP16\_3\_NLO PDF [18]. Due to symmetry, we assume that quantitatively the same effects happen for the  $W^- c$  process as well. The four studied scenarios were the following: (1) the vector boson is treated off-shell with spin-correlations in its decay (red continuous line in Fig. 1), (2) with spin-correlations retained in decay: the vector boson is produced on its mass shell using the narrow width approximation, *i.e.* changing the vector-boson propagator squared into a Dirac delta function

$$\frac{1}{(p_W^2 - m_W^2)^2 + m_W^2 \Gamma_W^2} \rightarrow \frac{\pi}{m_W \Gamma_W} \delta(p_W^2 - m_W^2). \quad (4)$$

This is illustrated by the blue continuous lines in Fig. 1. (3) no spin correlations in the vector-boson decay: randomly assigning direction to the lepton in the rest frame of the decaying boson. This is illustrated in Fig. 1 by curves with the green dashed line. In the last scenario, the vector boson is produced on-shell and stable in our event file and its decay (without spin-correlations) is delegated to PYTHIA 8 (blue dotted line in Fig. 1).

By taking a look at trends in Fig. 1, it can be seen that the effect of off-shellness is moderate at most but the presence of spin-correlations alters significantly the shape of the curves. Hence, for precision studies of this process, keeping the full propagator for the vector boson is only a marginal effect while retaining spin correlations is crucial. Thus, for our phenomenological studies, we keep spin correlations and treat the vector boson completely off-shell.

### 3.2. Comparisons at 7 TeV

At 7 TeV, the ATLAS Collaboration published results [10] both for  $W + D$ -meson and  $W + j_c$  cases, where  $j_c$  is a charm-tagged jet present in the final state. In this study, the  $W$  is analyzed in its leptonic decay channel and the absolute value of the charged lepton pseudorapidity is measured.

The analysis asks for an isolated lepton<sup>2</sup> in the final state with  $p_{T,\ell} > 20$  GeV and  $|\eta_\ell| < 2.5$ , a minimum of 25 GeV missing transverse energy, the  $W$  mass window is bound from below such that  $m_{T,W} > 40$  GeV.

For the  $D$ -meson production, at least one  $D$ -meson is required with  $p_T > 8$  GeV and  $|\eta_D| < 2.2$ . As for the charmed-jet analysis, jet recombination is done with the anti- $k_T$  jet algorithm with  $R = 0.4$  and requires strictly one charmed jet such that  $p_{T,j_c} > 25$  GeV in the central region ( $|\eta_{j_c}| < 2.5$ ). In the charmed-jet analysis, a charmed hadron has to be present with  $p_T > 5$  GeV.

---

<sup>2</sup> For details on the isolation requirements, see Section 4.1 of Ref. [10].

In Fig. 2, the pseudorapidities are depicted for  $D$ -meson production for the antilepton and the lepton, respectively. For illustrative purposes, we chose the ABMP16 PDF set. To assess uncertainties of our theoretical predictions, non-physical scales were varied around the central choice ( $\mu_0 = H_T/2$ ) and separately the PDF uncertainties were also evaluated by creating predictions with each member of the PDF set. For both  $D^-$ - and  $D^+$ -meson production, the scale uncertainty band amounts to  $\mathcal{O}(10\%)$  of the cross section, while the uncertainty coming from the PDF uncertainty is modest with a band width of 4%. For both  $D$ -mesons, the predictions describe the measurements really well. All the results shown in the pictures are based on the ATLAS A14 tune in PYTHIA 8. The same comparisons were carried out with the Monash tune as well without any significant change in our predictions. By comparing central lines of our predictions at hadron level with the two tunes, we found less than a 10% difference.

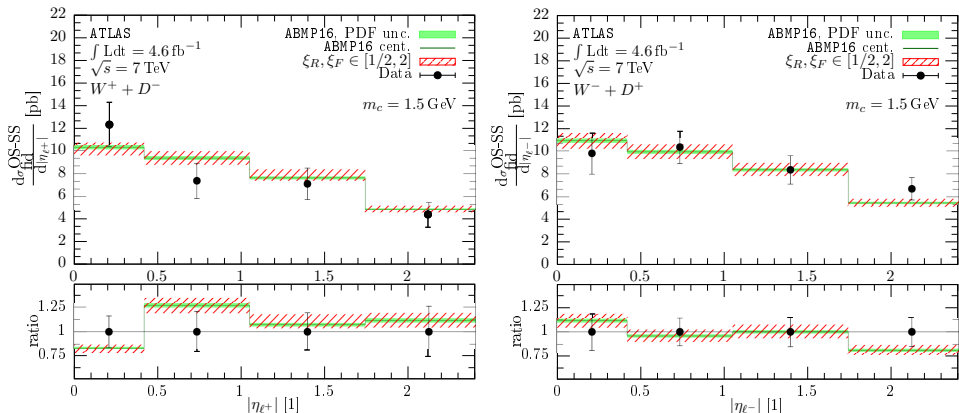


Fig. 2. Pseudorapidities for the produced antilepton (left-hand side) and lepton (right-hand side) using the  $D$ -meson analysis of ATLAS and comparing our predictions to actual ATLAS data taken at 7 TeV.

Our generated events were also used to make predictions for charmed-jet production at 7 TeV using the corresponding ATLAS analysis. Our predictions and comparison to data using this setup can be found in Fig. 3. We note that the experimental measurement has smaller relative errors compared to the  $W + D$  case. Even in this case, we found agreement with data. Predictions well describe the shape of the measured distributions. Pseudorapidity distributions are integrated into the transverse momentum of the charmed jet with a cut of  $p_{T,j_c} > 25$  GeV. Due to the one order of magnitude difference between the scale of the charm-quark mass and the minimal jet transverse momentum, the mass scale seems less important, though keeping the charm quark massive, the remaining Sudakov logarithms serve as a pos-

sible source of uncertainty in the three-flavor scheme being large and needing resummation at high values of the jet transverse momentum. From our results and the good level of agreement with data, the missing resummation effects seem to be heavily suppressed. It will be interesting to see the level of agreement as more data is accumulated resulting in smaller uncertainty for the measurement and after including NNLO QCD corrections to decrease the dependence on non-physical scales. From the current uncertainty band related to non-physical scales, a drastic decrease in band width is not expected, the only possibility is a slight change of normalization which can increase the discrepancy when accompanied by a reduction of measurement uncertainty.

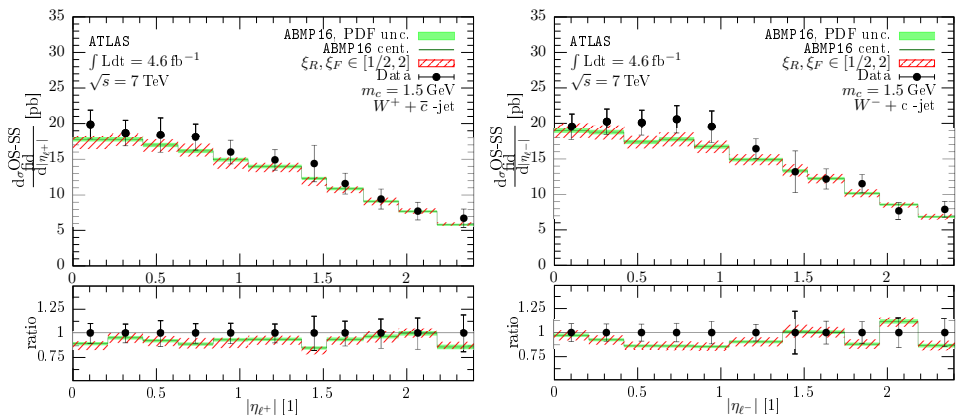


Fig. 3. Pseudorapidities for the produced antilepton (left-hand side) and lepton (right-hand side) using the charmed-jet analysis of ATLAS and comparing our predictions to ATLAS data taken at 7 TeV.

### 3.3. Comparisons at 13 TeV

At 13 TeV, the CMS Collaboration performed measurements for associated  $D$ -meson ( $D^*(2010)^\pm$ ) production [11]. To identify the leptonically decayed  $W$  boson, an isolated muon was required in the central region ( $p_{T,\mu} > 26$  GeV and  $|\eta_\mu| < 2.4$ ) with accompanying missing energy.

In the CMS analysis, the produced  $D^*(2010)$ -meson is required to be central ( $|\eta_{D^*(2010)}| < 2.4$ ) and allowing for very low transverse momentum ( $p_{T,D^*(2010)} > 5$  GeV). The minimal transverse momentum being very close to the charm-quark mass makes observations sensitive to this mass scale. For this collider energy, we made predictions [19] with three different PDF sets (ABMP16, CT18NLO, and CT18NLOZ) and two different PYTHIA 8 tunes (ATLAS A14 and Monash). Among the various ABMP16 PDF sets, the one was chosen which corresponds to the three-flavor number scheme.

This allowed us to perform a detailed study including PDF and scale uncertainty analysis. Five-flavor PDFs can also be used in three-flavor number scheme calculations if proper conversion takes place (for details see appendix of Ref. [19]). The correction factor only vanishes if the renormalization and factorization scales coincide. This made it possible to use the five-flavor CT18NLO and CT18NLOZ PDFs in our study and to obtain the corresponding PDF uncertainties.

Our predictions compared to CMS data using the ABMP16 PDF set and the ATLAS A14 tune are depicted in Fig. 4. As it can be seen from the plots, the agreement with data is good even at this energy. The scale uncertainty band is  $\mathcal{O}(10\%)$  wide and the corresponding PDF uncertainty band is around 4%. It is interesting to see how the level of agreement will change as more data is collected and/or higher-order corrections are taken into account in the theory predictions. Since the minimal transverse momen-

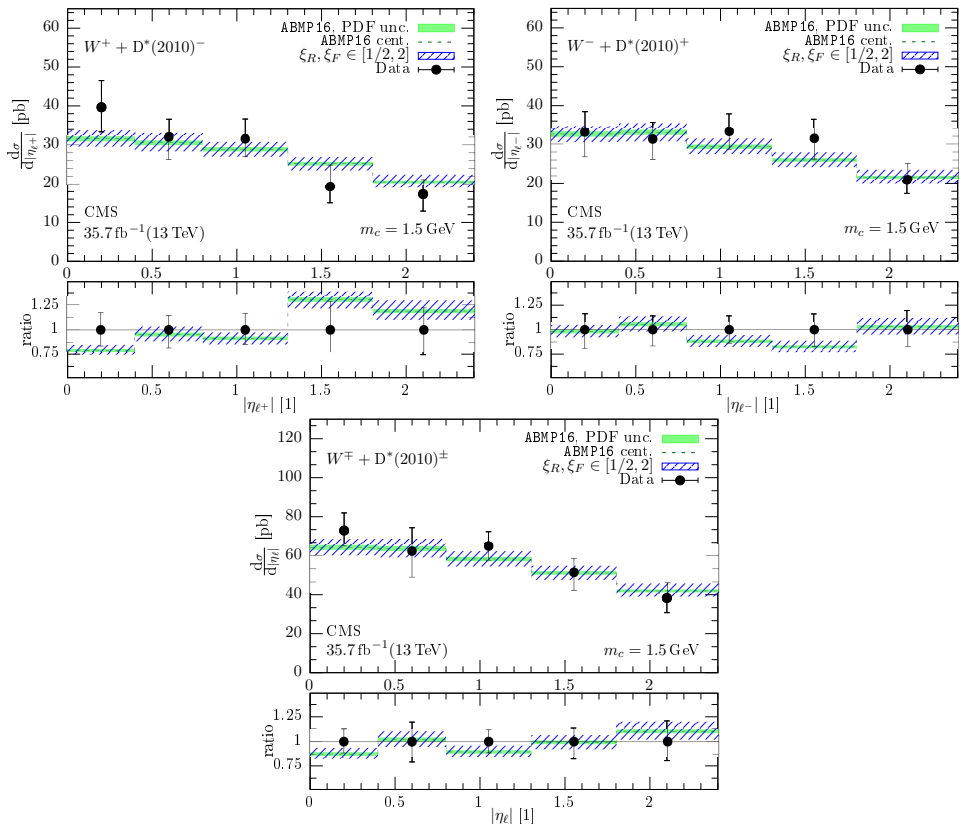


Fig. 4. Pseudorapidities for the produced antilepton (upper left-hand side), lepton (upper right-hand side) and these two combined (lower plot) using the  $D$ -meson analysis of CMS and comparing our predictions to CMS data taken at 13 TeV.

tum has the same scale as the charm-quark mass and because the Sudakov peak of the transverse momentum distribution peaks around that value, the pseudorapidity distributions receive large contributions from low- $p_T$  regions hence mass effects are important for this kind of studies.

#### 4. Conclusions

In these proceedings, we gave a brief account of our recent work where we compared hadron-level predictions for  $W$ +charm accurate at NLO in QCD with the experimental data taken by the ATLAS and CMS collaborations at 7 TeV and 13 TeV, respectively. We analysed the dependence of our results upon the variation of factorization and renormalization scales. We also generated predictions for a number of different PDF sets and assessed the internal uncertainties related to each set. This allowed us to provide solid estimates of the dominant theoretical uncertainties for the process at hand. Experiments conducted measurements for both  $D$ -meson and charmed-jet production and for all cases and at both energies, we were able to find agreement with experimental data. PDFs are important ingredients of prediction making for the LHC processes. To have high-precision PDFs is crucial for the success of the LHC program. Refining sea-quark PDFs is a major challenge because it needs processes which are well under control from the theory side and high-accuracy measurements can be made. The  $Wc$  process provides an opportunity to refine PDF fits to result in better uncertainties for  $s$  and  $\bar{s}$  distributions. Our predictions equipped with ATLAS and CMS data can be used to perform PDF fits narrowing down sources of uncertainty for sea-quark flavors.

This work was supported in part by the National Science Foundation under grant No. NSF PHY-1748958, by the grant K 125105 of the National Research, Development and Innovation Fund in Hungary, and by Bundesministerium für Bildung und Forschung (contract 05H18GUCC1).

#### REFERENCES

- [1] xFitter Developers' Team (H. Abdolmaleki *et al.*), «Probing the strange content of the proton with charm production in charged current at LHeC», *Eur. Phys. J. C* **79**, 864 (2019), [arXiv:1907.01014](https://arxiv.org/abs/1907.01014) [hep-ph].
- [2] M.V. Garzelli, «QCD opportunities with forward neutrinos during the HL-LHC phase», poster presentation at the APS 2021 April Meeting Quarks to Cosmos, 2021.

- [3] W.T. Giele, S. Keller, E. Laenen, «QCD corrections to W boson plus heavy quark production at the Tevatron», *Phys. Lett. B* **372**, 141 (1996), [arXiv:hep-ph/9511449](#).
- [4] J.M. Campbell, R.K. Ellis, W.T. Giele, «A multi-threaded version of MCFM», *Eur. Phys. J. C* **75**, 246 (2015), [arXiv:1503.06182 \[physics.comp-ph\]](#).
- [5] J. Alwall *et al.*, «The automated computation of tree-level and next-to-leading order differential cross sections, and their matching to parton shower simulations», *J. High Energy Phys.* **1407**, 079 (2014), [arXiv:1405.0301 \[hep-ph\]](#).
- [6] M. Czakon, A. Mitov, M. Pellen, R. Poncelet, «NNLO QCD predictions for W + c-jet production at the LHC», *J. High Energy Phys.* **2106**, 100 (2021), [arXiv:2011.01011 \[hep-ph\]](#).
- [7] CDF Collaboration (T. Aaltonen *et al.*), «First Measurement of W Boson Production in Association with a Single Charm Quark in  $p\bar{p}$  Collisions at  $\sqrt{s} = 1.96$  TeV», *Phys. Rev. Lett.* **100**, 091803 (2008), [arXiv:0711.2901 \[hep-ex\]](#).
- [8] D0 Collaboration (V.M. Abazov *et al.*), «Measurement of the ratio of the  $p\bar{p} \rightarrow W + c$ -jet cross section to the inclusive  $p\bar{p} \rightarrow W + \text{jets}$  cross section», *Phys. Lett. B* **666**, 23 (2008), [arXiv:0803.2259 \[hep-ex\]](#).
- [9] CDF Collaboration (T. Aaltonen *et al.*), «Observation of the Production of a W Boson in Association with a Single Charm Quark», *Phys. Rev. Lett.* **110**, 071801 (2013), [arXiv:1209.1921 \[hep-ex\]](#).
- [10] ATLAS Collaboration (G. Aad *et al.*), «Measurement of the production of a W boson in association with a charm quark in pp collisions at  $\sqrt{s} = 7$  TeV with the ATLAS detector», *J. High Energy Phys.* **1405**, 068 (2014), [arXiv:1402.6263 \[hep-ex\]](#).
- [11] CMS Collaboration (A.M. Sirunyan *et al.*), «Measurement of associated production of a W boson and a charm quark in proton–proton collisions at  $\sqrt{s} = 13$  TeV», *Eur. Phys. J. C* **79**, 269 (2019), [arXiv:1811.10021 \[hep-ex\]](#).
- [12] LHCb Collaboration (R. Aaij *et al.*), «Study of W boson production in association with beauty and charm», *Phys. Rev. D* **92**, 052001 (2015), [arXiv:1505.04051 \[hep-ex\]](#).
- [13] P. Nason, «A new method for combining NLO QCD with shower Monte Carlo algorithms», *J. High Energy Phys.* **0411**, 040 (2004), [arXiv:hep-ph/0409146](#).
- [14] S. Frixione, P. Nason, C. Oleari, «Matching NLO QCD computations with parton shower simulations: the POWHEG method», *J. High Energy Phys.* **0711**, 070 (2007), [arXiv:0709.2092 \[hep-ph\]](#).
- [15] S. Alioli, P. Nason, C. Oleari, E. Re, «A general framework for implementing NLO calculations in shower Monte Carlo programs: the POWHEG BOX», *J. High Energy Phys.* **1006**, 043 (2010), [arXiv:1002.2581 \[hep-ph\]](#).

- [16] T. Sjöstrand, «The PYTHIA event generator: Past, present and future», *Comput. Phys. Commun.* **246**, 106910 (2020), [arXiv:1907.09874 \[hep-ph\]](#).
- [17] G. Bevilacqua *et al.*, «HELAC-NLO», *Comput. Phys. Commun.* **184**, 986 (2013), [arXiv:1110.1499 \[hep-ph\]](#).
- [18] S. Alekhin, J. Blümlein, S. Moch, «NLO PDFs from the ABMP16 fit», *Eur. Phys. J. C* **78**, 477 (2018), [arXiv:1803.07537 \[hep-ph\]](#).
- [19] G. Bevilacqua, M.V. Garzelli, A. Kardos, L. Toth, « $W$  + charm production with massive  $c$  quarks in PowHel», [arXiv:2106.11261 \[hep-ph\]](#).